Fat-Water Separation in Alternating Repetition Time (ATR) Balanced SSFP

T. Cukur[1], and D. G. Nishimura[1]

[1]Electrical Engineering, Stanford University, Stanford, CA, United States

Introduction: Balanced steady-state free precession (SSFP) sequences can achieve high-resolution imaging with high signal-to-noise ratio (SNR) efficiency. Because SSFP leads to bright fat signal, methods for fat suppression have been of interest. Several methods for shaping the frequency response of SSFP were proposed, including FEMR [1], LCSSFP [2] and fat-suppressing alternating repetition time (ATR) SSFP [3]. The wedge-shaped stop-bands of these methods worsen the spectral selectivity and the resulting fat suppression in the presence of field inhomogeneities. In this work, a new method is proposed that combines in-phase and out-of-phase ATR images to yield fat and water images. Robust fat suppression can be achieved even in the presence of relatively high field variations, as the created stop-band is close to a perfect null.

Theory: In ATR SSFP, two different repetition times TR_1 and TR_2 are used consecutively as shown in Fig. 1.a. A stop-band around the fat resonant frequency can be created by carefully choosing the ratio $\tau = TR_2/TR_1$ and the phase cycling scheme. For fat suppression at 1.5 T, the condition $TR_1+TR_2 = 4.6$ ms should be met as it determines the separation between the pass- and stop-bands [3]. The phase of the RF2 pulse should be $\varphi_2 = 360^o\tau/(1+\tau)$ to place the null on the fat resonance. The magnetization profile with $TR_1/TR_2 = 3.45/1.15$ ms and a $(0\text{-}90\text{-}180\text{-}270)^o$ phase cycling is displayed in Fig. 1.b. The portion of the stop-band at higher frequencies (just to the right of the null) is out-of-phase and the other portion is contrarily in-phase with the signal at water resonance.

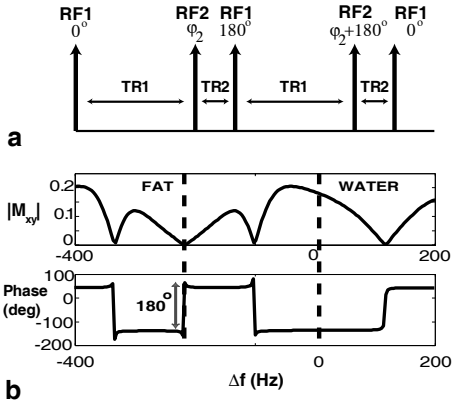

*Figure 1. **a:** RF pulses and the phase cycling scheme for an ATR sequence. **b:** The magnetization profile for fat-suppressing ATR assuming T1/T2=1000/200 ms.*

The in-phase portion can be extended by shifting the stop-band null to higher frequencies by decreasing φ_2, which also shapes the profile around the fat-resonance into a relatively flat band. Similarly, increasing φ_2 shifts the null to lower frequencies and extends the out-of-phase portion. For $\varphi_2 = 180^o/(1+\tau)$, the band around the fat-resonance is entirely out-of-phase and for $\varphi_2 = 180^o\tau/(1+\tau)$, it is entirely in-phase with the pass-band. Figures 2.a,b show the resulting magnetization profiles. The flat phase of the pass-band signal, which does not depend on T1/T2, τ or the flip angle, is slightly different for the in-phase and out-of-phase spectra. A summation of the profiles after removing this phase difference leads to the water image whereas the fat image is obtained by subtraction as shown in Fig. 2.c,d. The relatively flat shape of the in-phase and out-of-phase magnitude profiles over the stop-band leads to almost perfect cancellation of the fat signal.

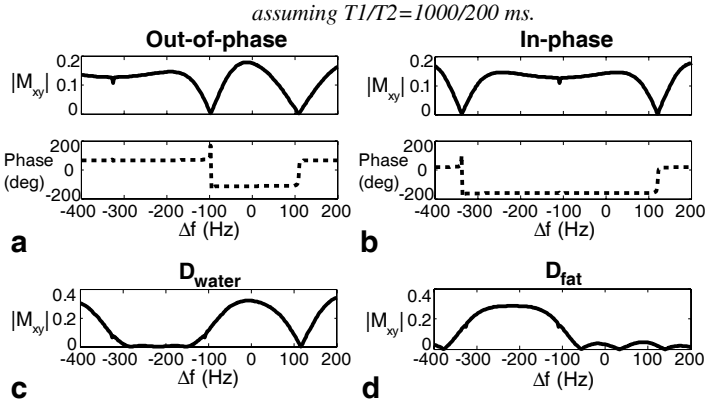

*Figure 2. The magnetization profile for $TR_1/TR_2 = 3.45/1.15$ ms, $\alpha = 60^o$, T1/T2 = 1000/200 ms and **a:** $\varphi_2 = 135^o$ (out-of-phase), **b:** $\varphi_2 = 45^o$ (in-phase). The **(c)** water-only and the **(d)** fat-only profiles after summation and subtraction of in-phase and out-of-phase images respectively.*

Results and Discussion: The ratio of the mean of the pass-band signal around the water-resonance to that of the stop-band signal around the fat-resonance within a ±80 Hz window can be computed for a range of T1/T2, TR_2/TR_1 values and flip angles as displayed in Fig. 3. The ratio is relatively insensitive to the T1/T2 ratio, whereas a τ value within the interval [0.25 0.4] yields the most robust suppression. Higher flip angles result in better stop-band signal reduction due to the increased flatness of the in-phase and out-of-phase profiles. Deviations from the condition $TR_1+TR_2 = 4.6$ ms are also tolerable; however, the spacing between the centers of the pass- and stop-bands will be $1/(TR_1+TR_2)$, reducing the width of the stop-band. The method improves the applicability of fat-suppressed SSFP imaging by allowing the prescription of a wide range of TR_1, TR_2 values and flip angles.

3D ATR SSFP images of a healthy volunteer's calf were acquired on a 1.5 T GE Signa Excite scanner. The acquisition parameters were: $\alpha = 60^o$, $TR_1/TR_2/TE = 3.45/1.15/1.7$ ms, 26 cm FOV, 1 mm isotropic resolution, ±125 KHz BW, $\varphi_2 = 135^o$ for the out-of-phase image, $\varphi_2 = 45^o$ for the in-phase image and a total acquisition time of 2:30. The in-phase and out-of-phase images, the resulting water image and a water image obtained with the regular fat-suppressing ATR ($\varphi_2 = 90^o$) are displayed in Fig. 4 along with the corresponding maximum-intensity projections. The water image acquired with the proposed method shows more robust fat suppression than the fat-suppressing ATR image.

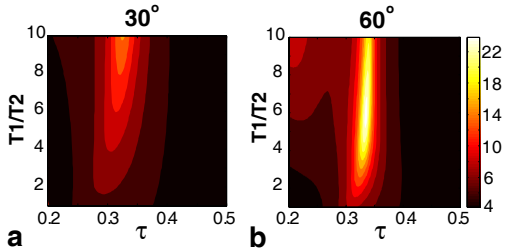

*Figure 3. The ratio of the mean pass-band signal to the mean stop-band signal for a range of T1/T2 and τ values with flip angles of **(a)** 30^o and **(b)** 60^o.*

References:

1. Vasanawala S, *et al.* MRM 42:876-83, 1999.

2. Vasanawala S, *et al.* MRM 43:82-90, 2000.

3. Leupold J, *et al.* MRM 55:557-65, 2006.

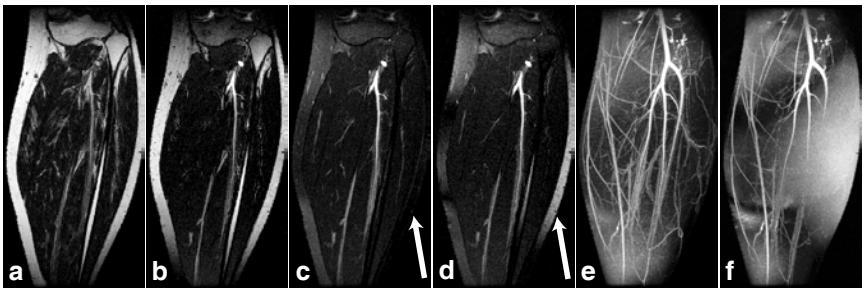

*Figure 4. The coronal slices for **(a)** out-of-phase, **(b)** in-phase acquisitions. Arrows point to the region where **(c)** the water-only image obtained by summation shows excellent fat suppression, whereas **(d)** the regular ATR image fails to suppress fat signal. The maximum-intensity projections are shown for **(e)** the water image in c and **(f)** the fat-suppressing ATR image in d.*